Electrostatic forces between a metallic tip and semiconductor surfaces

S. Hudlet, M. Saint Jean, B. Roulet, J. Berger, C. Guthmann

J. Phys I France **4** (1994) 1725-1742 NOVEMBER **1994**, PAGE 1725

Classification
Physics Abstracts
06.30L — 07.50 — 41.10D — 73.30 — 73.40Q

Electrostatic forces between a metallic tip and semiconductor surfaces

S. Hudlet, M. Saint Jean, B. Roulet, J. Berger and C. Guthmann

Groupe de Physique des Solides (*), Universités de Paris 7 et 6, T23, 2 place Jussieu 75251 Paris, France

(*Received 25 May 1994, accepted 25 July 1994*)

Résumé. — La Microscopie à Force Atomique en mode résonnant est un outil bien adapté à la mesure des caractéristiques locales des surfaces : par exemple, l analyse quantitative des forces électriques créées par l application d'une différence de potentiel entre la pointe conductrice du microscope et une surface en regard, permet de déterminer la capacité pointe/surface et le travail de sortie local de la surface. Toutefois cette analyse réclame un modèle adapté à chaque système. Cet article a pour but de calculer, dans un modèle géométrique simple, l interaction pointe/surface dans le cas d'une pointe métallique et d'une surface semiconductrice et de décrire ses variations en fonction du potentiel appliqué et de la distance pointe-surface Nos résultats montrent que ces forces présentent une grande richesse de comportements que nous avons associés aux différents régimes (accumulation, déplétion, inversion) du semiconducteur et que les modèles simples qui décrivent le système pointe/surface comme une capacité passive sont inappropriés.

Abstract. — The Atomic Force Microscope used in resonant mode is a powerful tool to measure local surface properties : for example, the quantitative analysis of the electrical forces induced by the application of an electrical tension between a conductive microscope tip and a surface in front allows the determination of the tip/surface capacitance and of the local surface work function. However, this analysis needs a well adapted model for each type of surface. In this paper, we calculate, with a simple geometrical model, the tip-surface interaction for a metallic tip and a semiconducting surface and we describe its variation with the applied tension and the tip/surface distance. Our results show different kinds of behaviour that we are able to associate with the different semiconductor regimes (accumulation, depletion, inversion). Therefore, it is not possible to describe this tip-surface system as a passive capacitance.

1. Introduction.

As device dimensions are reduced, the measurement of semiconductor electronic properties on a submicron scale becomes a challenge. In particular, the device performance depends

(*) CNRS UA17.

critically upon the dopant distribution on the nanometer scale. Unfortunately, the standard semiconductor characterization techniques, well adapted for large scales, do not allow such measurements. From this point of view, the development of the scanning probe microscopy promises a better characterization of these materials.

Among these kinds of microscopy the Atomic Force Microscopy in the Resonant Attractive mode (AFMR) offers the best opportunities. Indeed, it allows one to measure electrical parameters and topography simultaneously [1, 2].

In AFMR, a cantilever is excited at its resonance frequency Ω, a tip being located at its end. The force gradients between tip and sample shift this resonance frequency and induce a variation in the vibration amplitude of the cantilever. The resultant vibration is measured by using optical heterodyne detection and the signal is used in a feed-back loop to control the tip-surface sample distance. Topographic surface images are thus obtained at constant force gradient. Moreover, by applying a modulated bias voltage $V(\omega)$ between tip and sample, added capacitive forces are applied on the tip [2]. These forces induce cantilever oscillations at ω or 2 ω which can be measured. The magnitude of these induced oscillations depends on the intensity of the capacitive forces which are controlled by the electronic characteristics of the studied semiconductor surface (dopant concentration), thus, using a tip-sample interaction model, these quantities can be extracted from experimental results.

Several experiments, presenting instrumental opportunities, have been performed by using this new instrumentation. Different kinds of investigations have been carried out, essentially dopant concentration [3], surface photovoltage [4] and potentiometry measurements [5, 6].

Theoretical models have been developed to interpretate the tip-surface electrostatic forces quantitatively and to obtain precise information on the surface electronic properties.

A simple model has been proposed by Rugar *et al.* [2] in the case of metallic tip and metallic surface (called metal/metal case in the following). In this model, the tip-surface system is represented by a passive capacitance. They calculate the electrostatic energy of such a system and evaluate the forces using the virtual work method. They conclude that precise information about tip-surface capacity, contact potential and located charges on the surface can be obtained from these measurements.

This model has been extended by Abraham *et al* [3] to the case of a semiconductor surface (metal/semiconductor case). They have proposed a model in which the forces between metallic tip and semiconductor surface are directly extrapolated from the case of a metallic surface. The tip-surface system is modelled by an effective capacity C_{eff} due to the air gap, oxide and surface space-charge region near the semiconductor surface. Although this model introduces for the first time in AFM studies, the characteristic behaviour of semiconductors in an electric field, it unfortunately suffers some inconvenients and does not give the correct expression for the electrostatic force. In particular, the procedure used to derive the tip-surface force from the electrostatic energy only introduces the variations of the air capacitance with the tip-surface distance and neglects those of the space-charge distribution characteristic length.

A second model has been proposed by Huang *et al.* [7] who report a numerical calculation of the force. Their results are presented as formal and unclear expressions without intermediate derivations allowing a useful discussion.

In this paper, we propose a simple model to calculate the forces between a metallic tip and a semiconductor surface, a model which allows us to extract quantitative information from the experimental results. This model is developed in section 2. In section 3, we present the calculated variations of the induced forces with the externally controlled bias voltage and the tip-surface distance. The procedures required to extract the contact potential V_C, the tip-surface distance z and the local dopant concentration N_D from the experimental curves are described and discussed.

2. Electrostatic force between metallic tip and semiconductor sample.

The electrostatic force on a conducting tip held close to a semiconductor surface is calculated classically. The tip-surface system is modelled by two semi-infinite parallel plane surfaces, separated by a distance z (Fig. 1). Then the charge distribution in the semiconductor can be considered as one-dimensional.

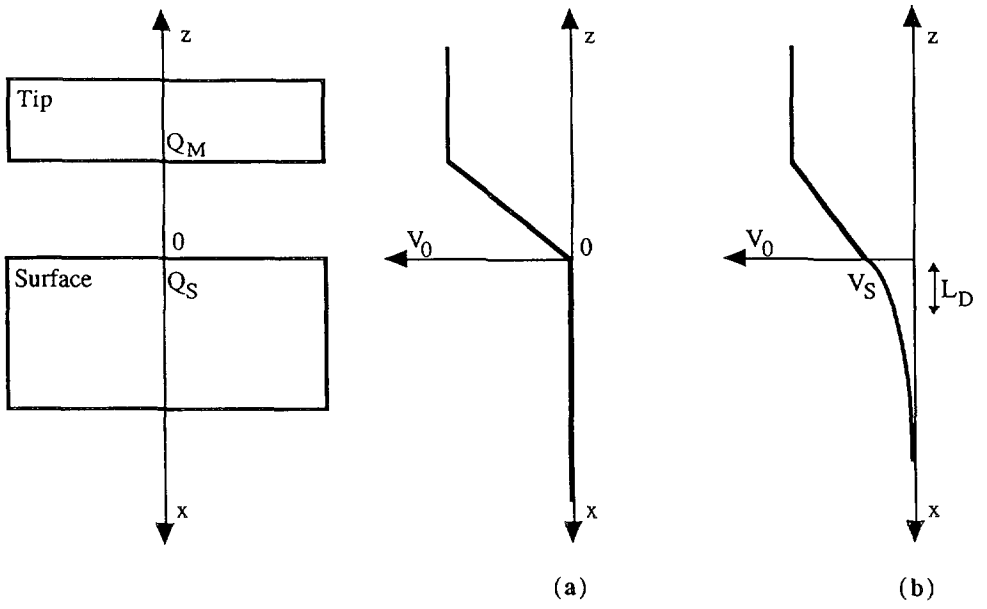

Fig. 1. — a) Metal tip/metal surface case. b) Metal tip/semiconductor surface.

Notice that these assumptions are very strong since the dimensions of the tip are very small and that lateral effects can be expected. However, this simple model is very useful to obtain a qualitative understanding of this physical situation and gives an efficient tool to interpret the experimental data semi-quantitatively.

Before calculating the electrostatic tip-surface forces in the case of the metal/semiconductor system, it is convenient to recall the case metal/metal in the same geometry (Fig. 1a).

The electrostatic energy of this system per unit area, U, is given by

$$U = \frac{1}{2} QV = \frac{Q^2}{2 C_1}$$

where Q is the charge per unit area located on the tip, V is the potential difference applied between the tip and the sample and $C_1 = \varepsilon_0/z$ is the associated capacitance per unit surface.

Following the virtual work method, the force applied on the tip is calculated as the derivative of U taken with respect to z, the electric charge Q being maintained constant.

The expression obtained for the attractive electrostatic force is given by

$$F = - \left(\frac{\partial U}{\partial z} \right)_Q = - \frac{Q^2}{2 \varepsilon_0} = - \frac{C_1^2 V^2}{2 \varepsilon_0} \qquad (1)$$

Moreover, if the potentiel difference V is given by

$$V = V_0 + V_C + V_1 \sin \omega t$$

where V_C is the local contact potentiel difference between the tip and the surface and the applied voltage consists of a dc component, V_0, and an ac component, V_1, with $V_1 \ll V_0$. Then this capacitive interaction induces three forces : a constant force F_0 and two sinusoidal forces $F_1(\omega)$ and $F_2(2\omega)$

$$F_0 = -\frac{C_1^2}{2\varepsilon_0}(V_0 + V_C)^2 \tag{2.1}$$

$$F_1(\omega) = -\frac{C_1^2}{\varepsilon_0}(V_0 + V_C)V_1 \sin \omega t \tag{2.2}$$

$$F_2(2\omega) = \frac{C_1^2}{4\varepsilon_0} V_1^2 \cos 2\omega t\,. \tag{2.3}$$

These forces induce cantilever oscillations at ω and 2ω. Some tip-surface electric characteristics can be obtained from the measurements of the magnitude of these oscillations. For instance, the amplitude of $F_1(\omega)$, which is proportional to $(V_0 + V_C)V_1$, offers the opportunity to measure the local contact potential difference between tip and surface. Following a procedure similar to the Kelvin method, the dc voltage level is varied until the ac induced vibration of the cantilever at ω is zero. At this point, $V_C = -V_0$. Thus, using this procedure, the local contact potential difference between a tip and a metallic surface can be evaluated with high spatial and voltage resolution.

In the metal/semiconductor case, the force calculation is less direct since the surface charges are not directly proportional to the applied bias voltage. The tip-surface capacitance is not passive and the force determination requires an adapted procedure.

In the following, the semiconductor is assumed to be n doped. The extension to the p-doped and n-p-doped semiconductor cases are very easy. Moreover, we will neglect the presence of an oxide at the surface and we will assume that there is no contact potential. The influence of these parameters on the different forces will be discussed later.

As in the metal/metal case, the first step is to calculate the total electrostatic energy U :

$$U = \frac{1}{2}\left(Q_M V_0 + \int_0^\infty \rho(x) V(x)\, dx\right)$$

where Q_M and V_0 are respectively the charge (per unit surface) and the voltage on the metallic tip, $\rho(x)$ and $V(x)$ are respectively the charge density (per unit area) and the potential voltage inside the semiconductor (Fig. 1b).

Introducing Poisson's equation $\nabla^2 V = -\frac{\rho}{\varepsilon}$ and taking advantage of the value of ∇V far from the semiconductor surface, $\nabla V(\infty) = 0$, U can be simply written as

$$U = \frac{Q_M V_0}{2} + \frac{Q_S V_S}{2} + \frac{\varepsilon}{2}\int_{V_S}^{0} \nabla V\, dV$$

where $Q_S = -Q_M = \int_0^\infty \rho(x)\, dx$ is the total charge in the semiconductor, V_S the semiconductor surface potential and ε its dielectric constant.

Moreover, the potential voltage continuity imposes a relation between V_0, V_S and Q_S .

$$V_0 = V_S - \frac{Q_S}{C_I} \tag{3}$$

The energy expression can be rewritten as

$$U = \frac{Q_S^2}{2 C_I} + \frac{\varepsilon}{2} \int_{V_S}^{0} \nabla V \, dV .$$

Using the virtual work method, the force applied to the tip is equal to $- \left(\frac{\partial U}{\partial z} \right)_{Q_S}$ and, since V_S only depends on Q_S (formula (6)) which is maintained constant, the applied force on the tip reduces to

$$F = - \frac{Q_S^2}{2 \varepsilon_0} \tag{4}$$

Notice that this expression is formally identical to those obtained in the case of metallic tip-metallic surface (Eq. (1)) and could directly be established by using the electrostatic pressure concept. However, it will be convenient to recall that, for metal-semiconductor system, Q_S is a complicated function of V_S and that this surface voltage, which depends on the tip-surface distance, has to be taken into account in the evaluation of the tip-surface force.

When the applied voltage V is a superposition of a constant voltage V_0 and a small modulation voltage $V_1 \sin \omega t$, forces are induced at frequencies ω and 2ω. The natural procedure to obtain the explicit expressions of the different forces is to expand the force F in a Taylor series

$$F(V_0 + V_1 \sin \omega t) = F(V_0) + V_1 \sin \omega t \frac{\partial F}{\partial V}(V_0) + \frac{(V_1 \sin \omega t)^2}{2} \frac{\partial^2 F}{\partial V^2}(V_0) + \cdots$$

and to exhibit terms independent of ω, proportional to $\sin \omega t$ and to $\cos 2 \omega t$. These terms correspond to F_0, $F_1(\omega)$ and $F_2(2\omega)$, respectively. By identification and only keeping the most significative terms, the expressions for the different forces are given by :

$$F_0 = F(V_0) \tag{5.1}$$

$$F_1(\omega) = \frac{\partial F}{\partial V}(V_0) V_1 \sin \omega t \tag{5.2}$$

$$F_2(2\omega) = - \frac{\partial^2 F}{\partial V^2}(V_0) \frac{V_1^2}{4} \cos 2 \omega t . \tag{5.3}$$

In this framework, the forces F_0, $F_1(\omega)$ and $F_2(2\omega)$ can be expressed as a function of Q_S and its derivatives with respect to V_S.

$$F_1(\omega) = V_1 \sin \omega t \left(\frac{\partial F}{\partial Q_S} \frac{\partial Q_S}{\partial V_S} \frac{\partial V_S}{\partial V} \right) (V = V_0) .$$

In this expression, the variations of V_S with the external potential voltage can be expressed with the air gap and space-charge capacities, C_I and C_D

$$\left(\frac{\partial V_S}{\partial V} \right) (V = V_0) = \frac{C_I}{C_I + C_D} \quad with \quad C_D = - \frac{\partial Q_S}{\partial V_S}$$

The final expression of $F_1(\omega)$ is :

$$F_1(\omega) = \frac{Q_S}{\varepsilon_0} \frac{C_I C_D}{C_I + C_D} V_1 \sin \omega t .$$

Following the same procedure, we can calculate the expression of the force at 2ω.

$$F_2(2\omega) = - \left(\frac{C_I}{C_I + C_D} \right)^3 \left\{ \frac{\varepsilon_0}{z^2} \left(\frac{C_D}{C_I} \right)^3 + \frac{1}{2\varepsilon_0} \frac{\partial^2 Q_S^2}{\partial V_S^2} \right\} \frac{V_1^2}{4} \cos 2\omega t .$$

3. Different physical regimes.

To evaluate the different forces, it is necessary to calculate Q_S and its different derivatives as a function of external bias voltage V_0 and tip-surface distance z.

The first step consists of calculating the semiconductor charge Q_S as a function of the semiconductor surface potential V_S. In order to determine $Q_S(V_S)$, Poisson's equation is integrated and the Gauss theorem is used to connect the charge inside the semiconductor with the electric field at the semiconductor surface. In the case of n-doped semiconductors, the expression of Q_S *versus* V_S is given by equation (8) :

$$Q_S = - \operatorname{sgn}(u) \frac{kT}{q} \frac{\varepsilon}{L_D} \left(e^u - u - 1 + \frac{n_i^2}{N_D^2} (e^{-u} + u - 1) \right)^{1/2} \tag{6}$$

where $u = \dfrac{qV_S}{kT}$, $L_D = \left(\dfrac{\varepsilon kT}{2 N_D q^2} \right)^{1/2}$, N_D, n_i and ε are respectively the dopant density, the intrinsic carrier density and the dielectric constant of the semiconductor, $q(>0)$ the electron charge magnitude.

In a second step, the continuity potential equation (3) is introduced to express the relation between V_0 and V_S .

$$V_0 = V_S - \frac{Q_S}{C_I} \tag{3}$$

Using these two equations, a unique $V_S(V_0, z)$ can numerically be calculated for each set of (V_0, z). Then, in a backforward procedure, this value is used to evaluate Q_S, its derivatives and the corresponding forces.

Before we present and discuss the variations of these forces with the external parameters (V_0, z), it is convenient to keep in mind the various physical situations that can be met, each of them corresponding to particular variations of Q_S, V_S and finally of the forces *versus* the external parameters (V_0, z).

Different regimes can be identified which correspond first to the different kinds of behaviour of Q_S *versus* V_S (accumulation, depletion and inversion regimes), and second to the relative magnitude of the potential decreases in the semiconductor V_S and in the air gap $-Q_S/C_I$ [9].

3.1 FOR VERY SMALL SURFACE VOLTAGE, $|V_S| < kT/q$, REGIMES R1 AND R2. — In these regimes, the charge in semiconductor is directly proportional to u :

$$Q_S \approx - \frac{kT}{q} \frac{\varepsilon}{\sqrt{2} L_D} \left(1 + \frac{n_i^2}{N_D^2} \right)^{1/2} u \approx - \frac{\varepsilon}{\sqrt{2} L_D} V_S \tag{7}$$

because n_i ($\approx 10^{16}$ m^{-3}) is much smaller than N_D ($\approx 10^{20}$ 10^{24} m^{-3}).

Then, by using (3), u is always proportional to V_0 since

$$V_0 \approx \left(1 + \frac{\varepsilon}{\varepsilon_0} \frac{z}{\sqrt{2}\, L_D}\right) V_S = - Q_S \left(\frac{\sqrt{2}\, L_D}{\varepsilon} + \frac{z}{\varepsilon_0}\right). \tag{8}$$

As $\varepsilon/\varepsilon_0 \approx 10$, if $z/L_D \gg 0.1$, the potential decrease inside the semiconductor can be neglected behind the applied voltage, the tip-surface capacity is reduced to the air capacity $C_1 = \varepsilon_0/z$ *(Regime R1)*. In contrast, if $z/L_D < 0.1$, the surface potential V_S cannot be neglected and the tip-surface system corresponds to an effective capacitance :

$$C_{eff} = \left(\frac{\sqrt{2}\, L_D}{\varepsilon} + \frac{z}{\varepsilon_0}\right)^{-1} \quad \textit{(Regime R2)}.$$

3.2 FOR LARGER POSITIVE SURFACE VOLTAGE, $u = qV_S/kT > 1$. ACCUMULATION REGIMES A1 AND A2. — In these regimes, the electrons (majority carriers in n-doped semiconductors) are attracted to the vicinity of the air-semiconductor interface, the resulting charge distribution is essentially located near this surface. In this accumulation regime,

$$Q_S \approx - \frac{kT}{q} \frac{\varepsilon}{L_D} e^{u/2}. \tag{9}$$

Then the relation (3) between u and V_0 is given by

$$V_0 \approx \frac{kT}{q} \left(u + \frac{\varepsilon}{\varepsilon_0} \frac{z}{L_D} e^{u/2}\right). \tag{10}$$

For not too small values of z/L_D, the contribution of the air capacitance is always larger than that of the semiconductor surface potential :

$$V_0 \approx \frac{kT}{q} \frac{\varepsilon}{\varepsilon_0} \frac{z}{L_D} \exp \frac{u}{2}, \qquad Q_S \approx - C_1 V_0 \tag{11}$$

In this regime *(accumulation regime A1)* u varies very slowly with V_0, and by inverting equation (11), can be assumed to be roughly equal to :

$$u_1 = 2 \operatorname{Ln} \left(\frac{qV_0}{kT} \frac{\varepsilon_0}{\varepsilon} \frac{L_D}{z}\right) \quad \text{(Fig. 2)}$$

In the following, the corresponding surface voltage is called $V_{S1}(z) = (kT/q)\, u_1$.

For very small values of z/L_D, the surface voltage contribution can be dominant in the continuity potential equation (3). In this regime *(accumulation regime A2)*,

$$u \approx qV_0/kT, \quad Q_S \approx - \frac{kT}{q} \frac{\varepsilon}{L_D} e^{qV_0/2kT} \tag{12}$$

The z/L_D value corresponding to the crossover between these two regimes can be evaluated and its order of magnitude is about 0.1 for the used V_0 (0, − 10 V), N_D values ($\approx 10^{20}$-10^{24} m^{-3}).

For negative surface voltage, we have two different kinds of behavior, according to whether V_S is smaller or higher than $-\Phi$, where $\Phi = 2 \frac{kT}{q} \operatorname{Ln} \left(\frac{N_D}{n_i}\right)$. This particular surface potential corresponds to the crossover between the values of $-u$ and e^{-u} in expression (6).

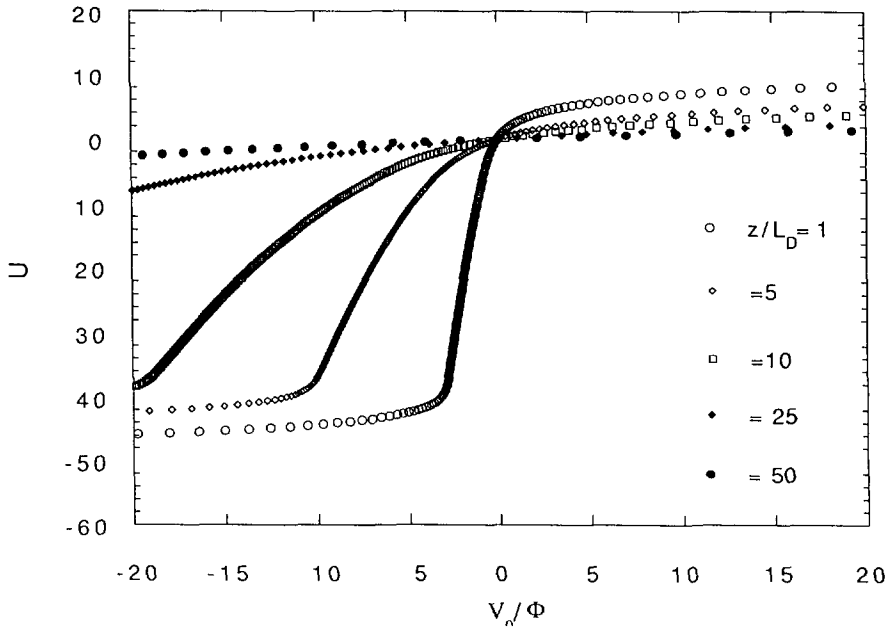

Fig. 2. — Variations of u *versus* V_0/Φ for different z/L_D ratio, $N_D = 10^{24}$ m^{-3}

3.3 FOR SMALL NEGATIVE VOLTAGE, $-\Phi < V_S < -kT/q$. DEPLETION REGIME D1 AND D2. — In this regime, the charge distribution is more expanded (over L_D), electrons are repelled from the vicinity of the interface leaving behind a space charge region of uncompensated ionised donor ions. In this depletion regime, Q_S and V_0 are related to u by the following expression :

$$Q_S \approx \frac{kT}{q}\frac{\varepsilon}{L_D}|u|^{1/2} \tag{13}$$

and

$$V_0 \approx -\frac{kT}{q}\left(|u| + \frac{\varepsilon}{\varepsilon_0}\frac{z}{L_D}|u|^{1/2}\right). \tag{14}$$

For large values of z/L_D (*Depletion regime D1*), the air capacitance contribution $-\frac{kT}{q}\frac{\varepsilon}{\varepsilon_0}\frac{z}{L_D}|u|^{1/2}$ is always larger than the semiconductor surface potential V_S, and :

$$V_0 \approx -\frac{kT}{q}\frac{\varepsilon}{\varepsilon_0}\frac{z}{L_D}|u|^{1/2}, \qquad Q_S \approx -C_I V_0 \tag{15}$$

As z/L_D decreases, a new regime appears in which the contribution associated to $-Q_S/C_I$ diminishes, and $|u|$ can be higher than $\frac{\varepsilon}{\varepsilon_0}\frac{z}{L_D}|u|^{1/2}$ Then, in this regime (*Depletion regime D2*) u is roughly proportional to V_0

$$V_0 \approx \frac{kT}{q}u, \qquad Q_S \approx \sqrt{\frac{kT}{q}}\frac{\varepsilon}{L_D}|V_0|^{1/2} \tag{16}$$

The z/L_D value corresponding to the crossover between these two regimes, given by $|u| \approx \frac{t}{\varepsilon_0}\frac{z}{L_D}|u|^{1/2}$, depends on V_0 and N_D. In the depletion regimes and for usual N_D values, z/L_D is about 0.5.

3.4 FOR $V_S < -\Phi$. INVERSION REGIMES I1 AND I2. — In this case, the holes (minority carriers) are attracted to a narrow region near the interface (inversion region) while inside the semiconductor the charge distribution is due to the charge of the ionised donors. As the voltage magnitude $|V_S|$ increases, a larger and larger fraction of the charge at the semiconductor surface will be holes. In this inversion regime, Q_S varies as

$$Q_S \approx \frac{kT}{q}\frac{\varepsilon}{L_D}\frac{n_i}{N_D}e^{|u|/2}. \tag{17}$$

The corresponding potential continuity equation is given by the following expression :

$$V_0 \approx -\frac{kT}{q}\left(|u| + \frac{\varepsilon}{\varepsilon_0}\frac{z}{L_D}\frac{n_i}{N_D}e^{|u|/2}\right). \tag{18}$$

As in the case of accumulation regimes, for not too small z/L_D values *(Inversion regime I1)*, the potential decrease outside the semiconductor is dominant

$$V_0 \approx -\frac{kT}{q}\frac{\varepsilon}{\varepsilon_0}\frac{z}{L_D}\frac{n_i}{N_D}e^{|u|/2} \qquad Q_S \approx -C_i V_0. \tag{19}$$

As is shown in figure 2, u varies slowly with V_0 and can be roughly considered as equal to $u_2 = -2\,\mathrm{Ln}\left|\frac{qV_0}{kT}\frac{\varepsilon_0}{\varepsilon}\frac{N_D}{n_i}\frac{L_D}{z}\right|$ In the following the corresponding surface voltage will be called $V_{S2}(z) = (kT/q)\,u_2$.

However, for small values of z/L_D, the surface potential contribution can be dominant. Then $u \approx qV_0/kT$ and Q_S is proportional to $e^{-qV_0/2kT}$ *(Inversion regime I2)*.

$$V_0 \approx \frac{kT}{q}u, \qquad Q_S \approx \frac{kT}{q}\frac{\varepsilon}{L_D}\frac{n_i}{N_D}e^{q|V_0|/2kT} \tag{20}$$

The z/L_D value corresponding to the crossover between these two regimes can be evaluated and is about 0.1 for the values of V_0 and N_D used.

In this discussion we have introduced two characteristic surface potentials, $|V_S| = kT/q$ and $V_S = -\Phi$. It is convenient to also introduce the external parameters V_0 and z corresponding to these potentials, noted $|V_0^{kT/q}|$ and V_0^{Φ} respectively, which are related by the following expression obtained from the potential continuity equation :

$$\begin{aligned} |V_0^{kT/q}|(z) &= \left[\frac{kT}{q} + \frac{z}{\varepsilon_0}Q_S\left(\frac{kT}{q}\right)\right] \\ V_0^{\Phi}(z) &= -\left[\Phi + \frac{z}{\varepsilon_0}Q_S(\Phi)\right]. \end{aligned} \tag{21}$$

Thus, according to the different regimes characterized by the values of V_0 and z/L_D, different variations with V_0 can be observed for Q_S and then for F and its derivatives. These various kinds of behaviour are summarized in table I In particular, it is important to

Table I.

	Regime R $\lvert u\rvert<1$		Regime A $u>1$		Regime I $u<q\phi/kT$		Regime D $q\phi/kT<u<1$	
	$Q_S = -\frac{\varepsilon}{\sqrt{2}L_D} V_S$ $V_0 = -Q_S\left(\frac{\sqrt{2}L_D}{\varepsilon} + \frac{z}{\varepsilon_0}\right)$		$Q_S = -\frac{kT}{q}\frac{\varepsilon}{L_D} e^{u/2}$ $V_0 = \frac{kT}{q}\left(u + \frac{\varepsilon}{\varepsilon_0} + \frac{z}{L_D} e^{u/2}\right)$		$Q_S = \frac{kT}{q}\frac{\varepsilon}{L_D}\frac{n_i}{N_D} e^{\lvert u\rvert/2}$ $V_0 = -\frac{kT}{q}\left(u + \frac{\varepsilon}{\varepsilon_0}\frac{z}{L_D}\frac{n_1}{N_D} e^{\lvert u\rvert/2}\right)$		$Q_S = \frac{kT}{q}\frac{\varepsilon}{L_D}\sqrt{\lvert u\rvert}$ $V_0 = -\frac{kT}{q}\left(u + \frac{\varepsilon}{\varepsilon_0}\frac{z}{L_D}\sqrt{\lvert u\rvert}\right)$	
	R1	**R2**	**A1**	**A2**	**I1**	**I2**	**D1**	**D2**
$\frac{z}{L_D}$	» 0 1	< 0.1	> 0.1	« 0.1	> 0.1	« 0.1	» 0.5	« 0.5
Q_S	$-C_I V_0$	$-C_{eff} V_0$	$-C_I(V_0-V_{S1})$	$-\frac{kT}{q}\frac{\varepsilon}{L_D} e^{\lvert qV_0\rvert/2kT}$	$-C_I(V_0-V_{S2})$	$\frac{kT}{q}\frac{\varepsilon}{L_D} e^{\lvert qV_0\rvert/2kT}$	$-C_I V_0$	$\sqrt{\frac{kT}{q}}\frac{\varepsilon}{L_D}\sqrt{\lvert V_0\rvert}$
$\lvert F_0\rvert$	$\frac{C_I^2}{2\varepsilon_0} V_0^2$	$\frac{C_{eff}^2}{2\varepsilon_0} V_0^2$	$\frac{C_I^2}{2\varepsilon_0}(V_0-V_{S1})^2$	$\frac{(kT)^2}{q^2}\frac{\varepsilon^2}{2\varepsilon_0 L_D^2} e^{\lvert qV_0\rvert/kT}$	$\frac{C_I^2}{2\varepsilon_0}(V_0-V_{S2})^2$	$\frac{n_i^2}{N_D^2}\frac{(kT)^2}{q^2}\frac{\varepsilon^2}{2\varepsilon_0 L_D^2} e^{\lvert qV_0\rvert/kT}$	$\frac{C_I^2}{2\varepsilon_0} V_0^2$	$\frac{kT}{q}\frac{\varepsilon^2}{L_D^2}\frac{1}{2\varepsilon_0} V_0$
$\frac{\lvert F_1\rvert}{V_1}$	$\frac{C_I^2}{\varepsilon_0}\lvert V_0\rvert$	$\frac{C_{eff}^2}{\varepsilon_0}\lvert V_0\rvert$	$\frac{C_I^2}{\varepsilon_0}(V_0-V_{S1})$	$\frac{kT}{q}\frac{\varepsilon^2}{2\varepsilon_0 L_D^2} e^{\lvert qV_0\rvert/kT}$	$\frac{C_I^2}{\varepsilon_0}\lvert V_0-V_{S2}\rvert$	$\frac{n_i^2}{N_D^2}\frac{kT}{q}\frac{\varepsilon^2}{2\varepsilon_0 L_D^2} e^{\lvert qV_0\rvert/kT}$	$\frac{C_I^2}{\varepsilon_0}\lvert V_0\rvert$	$\frac{kT}{q}\frac{\varepsilon^2}{L_D^2}\frac{1}{2\varepsilon_0}$
$\frac{4\lvert F_2\rvert}{V_1^2}$	$\frac{C_I^2}{\varepsilon_0}$	$\frac{C_{eff}^2}{\varepsilon_0}$	$\frac{C_I^2}{\varepsilon_0}$	$\frac{\varepsilon^2}{2\varepsilon_0 L_D^2} e^{\lvert qV_0\rvert/kT}$	$\frac{C_I^2}{\varepsilon_0}$	$\frac{n_i^2}{N_D^2}\frac{\varepsilon^2}{2\varepsilon_0 L_D^2} e^{\lvert qV_0\rvert/kT}$	$\frac{C_I^2}{\varepsilon_0}$	0

n-doped semiconductor

$$Q_S = \operatorname{sgn}(u)\frac{kT}{q}\frac{\varepsilon}{L_D}\left(e^u - u - 1 + \frac{n_i^2}{N_D^2}\left(e^{-u} + u - 1\right)\right)^{1/2} \qquad u=\frac{qV_S}{kT} \qquad L_D=\left(\frac{\varepsilon\, kT}{2N_D q^2}\right)^{1/2} \qquad V_0=V_S-\frac{Q_S}{C_I} \qquad C_I=\frac{\varepsilon_0}{z} \qquad C_{eff}=\left(\frac{\sqrt{2}L_D}{\varepsilon}+\frac{z}{\varepsilon_0}\right)^{-1}$$

notice that in some regimes, which can be reached experimentally, Q_S is not always proportional to V_0 and that the simple description using passive capacitance to describe the tip-surface system is inappropriate.

Figure 2 presents the previously discussed variations of u *versus* the voltage parameter V_0/Φ, for different values of the distance parameter z/L_D. In these numerical calculations, the semiconductor surface is a Si-n doped surface, $N_D = 10^{20}$ dopants/m^3 ($\Phi \sim 0.5$ V, $L_D \sim 275$ nm). For another dopant concentration, the curves have to be recalculated to obtain the absolute values of Φ and L_D but the main behaviour of $u(V_0, z)$ is very similar. In the following figures, the retained values for V_0/Φ and z/L_D correspond to a maximal applied voltage extension ± 10 V and a minimal distance tip-surface about 1 nm.

4. Numerical evaluations of F_0, F_1 and F_2.

In this section we present and discuss the variations of the different forces F_0, $F_1(\omega)$ and $F_2(2\omega)$ *versus* the bias voltage V_0, calculated for different values of the tip-surface distance and different dopant concentrations.

4.1 The static force F_0.

4.1.1 *Variations with applied voltage* V_0. — Figure 3 shows the theoretical dependence of F_0 with V_0. The results are obtained for three different dopant concentrations, $N_D = 10^{20}$ 10^{22}, 10^{24} m^{-3} corresponding respectively to $L_D = 275$, 27.5, 2.75 nm, and $\Phi = 0.5$, 0.75, 1 V. The tip-surface distance is equal to 10 nm (the surface area is arbitrarily taken equal to 10^{-2} μm^2).

For positive applied voltage, whatever the dopant concentration, F_0 presents rough quadratic variations as in the pure metallic case. For the selected ranges of distance and according to the voltage value, the system is in the different regimes R1 or A1, the accumulation regime A2 being reached only for $N_D = 10^{20}$ m^{-3}

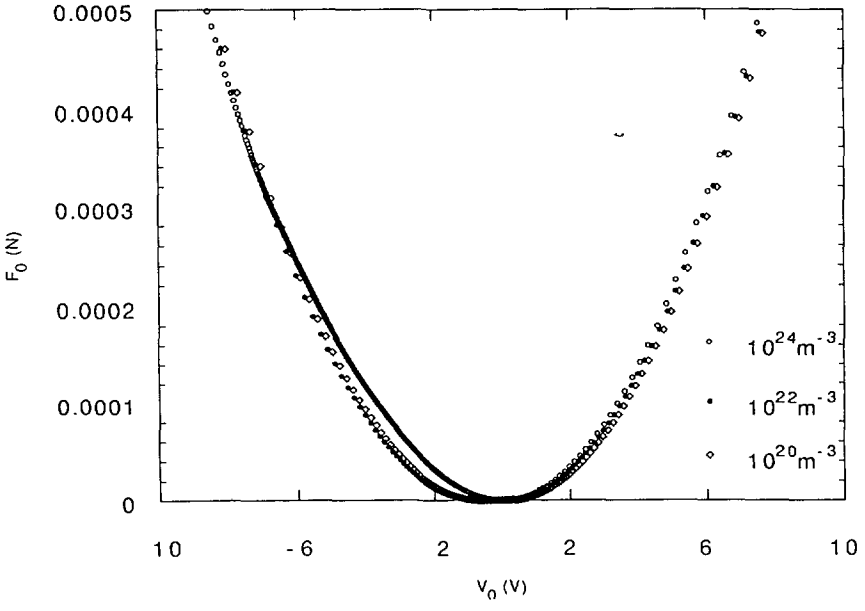

Fig. 3. — Variation of F_0 *versus* V_0 for different dopant concentrations.

For a small applied voltage, the system is in R1 regime. F_0, proportional to Q_S^2 varies as $(C_{eff}\, V_0)^2$ (Eq. (8)).

For a large voltage, the system is in A1 regime, F_0 is then equal to $C_I^2(V_0 - V_{SI})^2$ (Eq. (11). Notice that the presence of V_{SI} term induces a particular voltage « shift » $V_{SI}(z)$ with respect to the metal/metal case. For each F_0 curve, this shift increases as N_D and z/L_D decreases.

For negative bias voltage, the tip-surface system can be in the depletion or inversion regime. Using formula (21) the bias voltage V_0^{Φ} required to reach the inversion regime when $z = 10$ nm can be evaluated. For n-doped semiconductor with $N_D = 10^{24}$, 10^{22}, 10^{20} m^{-3}, it is about -9 V, -1.8 V and -0.6 V, respectively. Thus, for a small negative voltage, the semiconductor is in the depletion regime D1 if $N_D = 10^{24}$ m^{-3} whereas, according to the bias voltage regime, the system is rapidly in the inversion regime I1 for lower dopant concentrations. In these two regimes, Q_S is proportional to V_0 and the F_0 variations are roughly quadratic (Eqs. (15), (19)) the detail of the structures of the curves will be more evident, if one looks at the curves of the F_1 forces.

For a large negative bias voltage, the tip-surface system is in the inversion regime I1 whatever the dopant concentration. The situation is very similar to the previous accumulation regime. F_0 being proportional to $C_I^2(V_0 - V_{S2})^2$ and in a same way, some shifts can be observed. Moreover, from these results, we can notice that the curves F_0 are not symmetric with respect to $V_0 = 0$.

4.1.2 *Variations with the tip-surface distance.* — The variations of F_0 with the tip-surface distance ($z/L_D = 0.1$ 0.5, 2) for a given dopant concentration, $N_D = 10^{20}$ m^{-3}, are shown in figure 4.

For a positive bias voltage, the system is essentially in accumulation regime A1, Q_S is proportional to V_0 and F_0 variations are quadratic (Eq. (11)). The particular case of

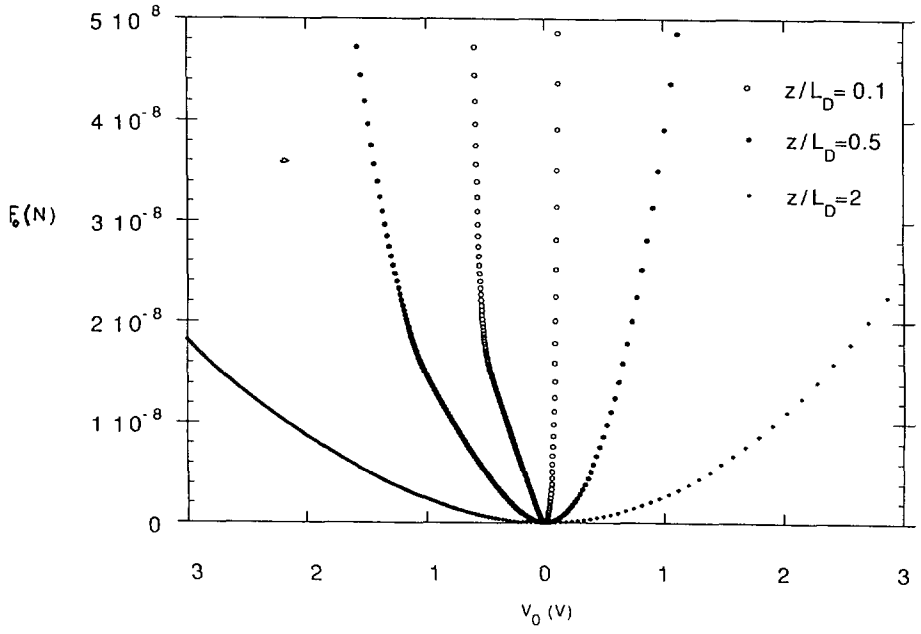

Fig. 4. — Variations of F_0 *versus* V_0 for different z/L_D ratio, $N_D = 10^{20}$ m^{-3}

$z/L_D = 0.1$ and small voltage (Accumulation regime A2) will be discussed more completely in the section related to F_1.

For $z/L_D = 2$, $V_0^{\Phi}(z) = -4$ V, then for the presented V_0 range (-3 V $< V_0 < 0$) the tip-surface system is in the depletion regime (D1 or R1), Q_S is proportional to V_0 and the variations of $F_0(V_0)$ are roughly quadratic (Eqs. (8), (15)). Note however that the curve is asymmetric with respect to $V_0 = 0$, this behaviour underlines the more rapid increase of $u(V_0, z)$ for $V_0 > 0$ than for $V_0 < 0$ (Fig. 2).

As the ratio z/L_D decreases, V_0^{Φ} decreases and is about -1.2, -0.6 V for $z/L_D = 0.5$ and 0.1, respectively. For large negative voltage, $V_0 < V_0^{\Phi}$, the system is in the inversion I1 regime, Q_S is proportional to V_0 and F_0 varies quadratically (Eq. (19)). In contrast, for $V_0 > V_0^{\Phi}(z)$, the system reaches the depletion D2 regime in which Q_S^2 varies as V_0 (Eq. (16)), then F_0 varies linearly with V_0. This effect is particulary evident on the $z/L_D = 0.1$ curve.

4.2 THE FORCE $F_1(\omega)$.

4.2.1 *Variations with applied voltage* V_0. — The variations of F_1 *versus* V_0 for different dopant concentrations and $z = 10$ nm are shown in figure 5.

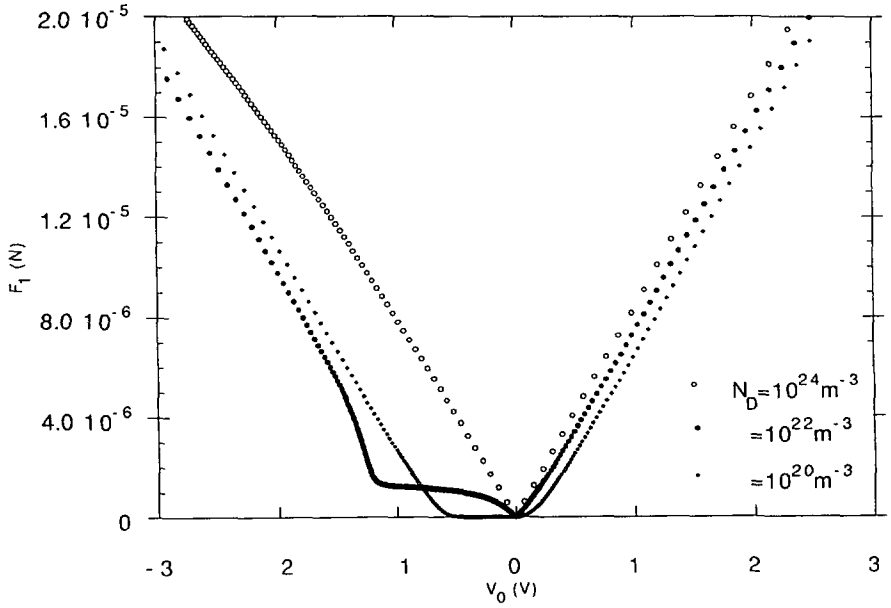

Fig. 5. — Variation of F_1 *versus* V_0 for different dopant concentrations. $z = 10$ nm.

For a large positive voltage, F_1 varies linearly with V_0, the tip-surface system is in the A1 or R1 regimes. The different curves are parallel but shifted with respect to the metallic case by $V_1(z)$, and can be discussed in a similar way as the F_0 curves. The slope of all these curves is proportional to C_1^2 as for a metal-metal system and is independent of the dopant concentration, in agreement with the accumulation picture. Notice that these curves reach the origin since we have neglected the effect of contact potential ; if we introduce the contact potential V_C which is similar to a modification of the potential origin, the curves will be shifted by $-V_C$.

Note however that for very small voltages, the system corresponding to $N_D = 10^{20}\ m^{-3}$ reaches the A2 regime in which Q_S varies as $\exp(qV_0/2\,kT)$ (Eq. (12)). This effect can be observed in the inset.

For negative voltages, the crossover from the depletion regime to the inversion regime also appears on the $F_1(\omega)$ curves. Since $F_1(\omega)$ is the first derivative of F_0 with respect to V_0, the non-quadratic behaviour in F_0 dependence will appear as a non-linear behavior in $F_1(\omega)$.

The most important effect is the presence of an elbow and that the applied voltage at which it appears depends on z/L_D. In fact, this elbow precisely corresponds to the regime transition, the applied potential V_0 being then equal to $V_0^{\Phi}(z)$ (the elbow corresponding to the curve $N_D = 10^{24}\ m^{-3}$ appears at $V_0 = -9$ V, out of the figure range). This behaviour can be qualitatively explained as follows : in the depletion regime, the effective distance between the mobile carriers in the metal and in the semiconductor is roughly equal to z augmented by the depletion length. As the magnitude of the applied voltage increases, the depletion region width increases and the effective capacitance decreases. Then, for a small applied voltage, $F_1(\omega)$ variation is smaller than in the metal/metal case. In contrast, when the inversion region is reached, the effective distance between the mobile carriers in the metal and in the semiconductor returns to z and $F_1(\omega)$ is similar to the metallic tip-metallic surface case. However, in the last case, the surface voltage V_S is not zero but equal to $V_2(z)$ which increases as z is reduced. This induces shifts in the F_1 curves.

For very small voltages corresponding to the R1 regime, we can observe that F_1 linearly varies with V_0 in a similar way as for large negative voltages for which the system is in inversion regime I1. Note that, in this regime, the curves $F_1(V_0)$ are roughly parallel and that their slopes $\dfrac{\partial F_1}{\partial V_0}$ $(V_0 = 0)$ are proportional to C_1^2.

Some others characteristic behaviours can be observed on these curves. For instance, for $N_D = 10^{22}\ m^{-3}$ and for V_0 about -1.8 V, a tip-surface distance equal to 10 nm corresponds to a regime very close to the inversion regime I2 in which F_1 varies as $\exp q|V_0|/kT$ (as shown in Fig. 5). For smaller voltages, the system is in the D2 depletion regime and F_1 corresponds to a roughly constant value, since in this regime F_0 is proportional to V_0.

4.2.2 *Influence of the tip-surface distance.* — The variations of F_1 *versus* V_0 for different values of z/L_D, $N_D = 10^{20}\ m^{-3}$, are shown in figure 6. It is interesting to observe that the variation of the elbow position with z/L_D is very sensitive to the tip-surface distance, its value decreasing with a decrease of the tip-surface distance z.

Moreover, the different kinds of behaviour of $F_1(V_0, z)$ *versus* z can be observed. For instance, for $V_0 = -0.6$ V, we can very precisely follow the different regimes crossed when the tip-surface distance increases. For $z/L_D = 0.05$, the tip-surface system is in the inversion regime I2 and $F_1(\omega)$ increases exponentially for $V_0 < V_0^{\Phi}(z)$ and is constant for $V_0 > V_0^{\Phi}(z)$. As z/L_D increases, the system reaches the depletion regime D2 for $z/L_D = 0.25$, and the regime D1 for $z/L_D > 0.5$. In the same time, the elbow is shifted towards the large negative voltage.

4.3 THE FORCE $F_2(2\,\omega)$. — Figure 7 presents the variations of $F_2(2\,\omega)$ *versus* voltage for different dopant concentrations, the tip-surface distance being equal to 10 nm. For a positive voltage, except for very small values, F_2 is roughly constant and equal to C_1^2/ε_0 and independent of N_D.

In constrast, for a negative voltage, these curves show different features, characterized by the dopant concentration and the tip-surface distance. As the bias voltage decreases,

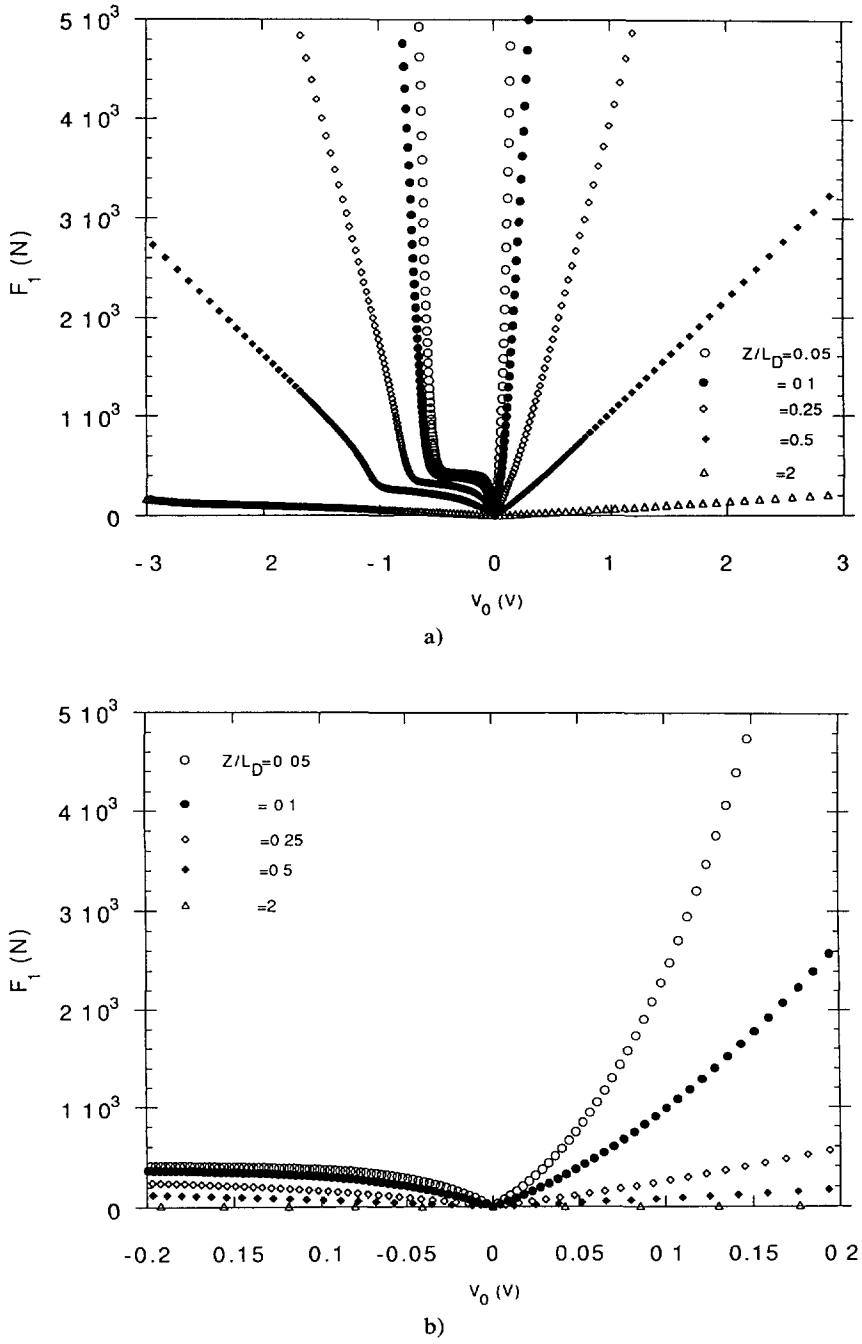

Fig. 6. — Variation of F_1 *versus* V_0 for different z/L_D ratio, $N_D = 10^{20}$ m^{-3}

$F_2(2\omega)$ progressively decreases as the system enters the depletion regime and reaches the inversion regime. The transition Depletion/Inversion regime is characterized by a strong « singularity » in the curve. For a very large negative voltage, in the inversion regime, F_2 is constant.

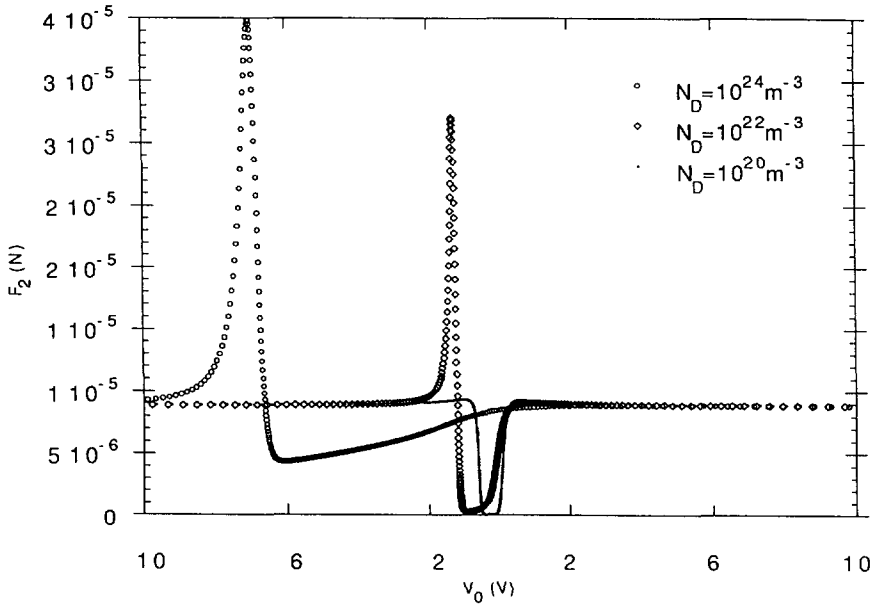

Fig. 7. — Variation of F_2 *versus* V_0 for different dopant concentrations, $z = 10$ nm.

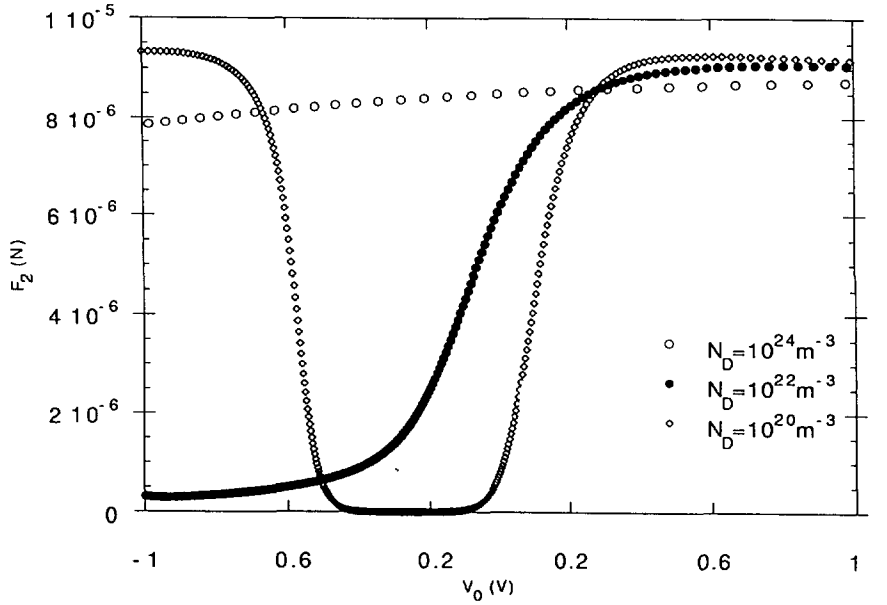

Fig. 8. — Variation of F_2 *versus* V_0 for different dopant concentrations, $z = 10$ nm for small applied voltage.

In particular, it is important to note that, for small values of V_0, $-1\ \mathrm{V} < V_0 < 1\ \mathrm{V}$, $F_2(2\omega)$ is very sensitive to the dopant concentration as shown in the inset, the $F_2(2\omega)$ magnitude increases with N_D.

4.4 QUANTITATIVE ANALYSIS OF ELECTRICAL FORCES. — Several physical quantities can be extracted from these presented curves.

The contact potential V_C between the tip and the surface can be obtained from the measurement of the voltage corresponding to $F_1(\omega) = 0$. In this situation, the applied potential V_0 is exactly equal to $- V_C$. Using a feed back loop asserving the applied voltage to fix $F_1(\omega) = 0$, the image of isocontact potential can be obtained.

The value of the tip-surface distance can be obtained from the measurement of $F_2(2\omega)$ for large positive applied voltage, since in this regime, this force is simply proportional to C_1^2 and is dopant concentration independent.

The local dopant concentration can be determined from different issues :

— If z is higher than L_D, the N_D values can be obtained from the measurements of $F_2(2\omega)$ at $V_0 = 0$ (at $V_0 = - V_C$ if we consider the contact potential) (Fig. 8). Using this opportunity, images of isoconcentrations can be performed.

— For small z/L_D, it seems easier to use the $F_1(\omega)$ curves. Indeed, we have shown that, in this case, the depletion/inversion transition is characterized by an elbow in the $F_1(\omega)$ curves. Since this feature appears when $V_0 = V_0^{\Phi}$, we can extract the dopant concentration from the measurements of the voltage position of this elbow.

5. Conclusion.

In this study, we have calculated the different electrostatic forces between the metallic tip of an AFMR microscope and an n-doped semiconductor surface separated by an air gap and submitted to an applied voltage. In particular, the variations of these forces *versus* the static applied voltage have been investigated.

This study shows that, in this system, the different force variations present many more various kinds of behaviour than those observed when the surface is metallic. Different regimes can be exhibited according to the values of the tip-surface distance and the static applied voltage.

These various regimes originate from the different behaviour of the semiconductor surface charge Q_S *versus* the surface voltage V_S which depends on the applied voltage and on the relative importance of the air gap contribution with respect to the potential decrease inside the semiconductor, characterised by the Debye length L_D.

Roughly speaking, we can conclude that for a fixed applied voltage, when the tip-surface distance z is much higher then L_D the system is roughly similar to the metal/metal case. In contrast when z is smaller than L_D, this simple model is not adapted and some features appear in the curves representing the variations of the forces *versus* the applied voltage. It will be important to keep these effects in mind to interpret the experimental results obtained with AFM microscopes since, in these experiments, the most commonly used tips are semiconductor tips and that there exists a contact potential between the tip and the surface, even without applied voltage. So, some features, associated with these effects, can appear in the force curves and in the images.

This study presents some limits however ; in our calculation, we have neglected the presence of an oxide layer on the semiconductor surface. However, this assumption does not qualitatively modify the present results, since its presence is in fact qualitatively similar to an effective reduction of the tip-surface distance with respect to the case without oxide. Moreover, in this model, the tip and the semiconductor surfaces are assumed to be parallel plates. This geometry does not correspond to the experimental configuration when the tip-surface distance is smaller than the tip curvature radius ($z < 100$ nm) ; in this case the tip is better described by an ellipsoid electrode. Nevertheless our simple model, which can be

extended to ellipsoid/plate geometry, offers the opportunity to provide a useful semiquantitative understanding of the electrostatic forces which are accounted for in the AFMR.

References

[1] Martin Y., Abraham D. W., Wickramasinghe H. K., *Appl. Phys Lett* **52** (1988) 1103.

[2] Terris B. D., Stern J. E., Rugar D., Mamin H. J., *Phys. Rev Lett* **63** (1989) 2669.

[3] Abraham D. W., Williams C., Slinkman J., Wickramasinghe H. K., *J Vac. Sci Technol* **B 9** (1991) 703.

[4] Weaver J. M. R., Wickramasinghe H. K., *Vac Sci Technol.* **B 9** (1991) 1562, and references which are therein.

[5] Nonnenmacher M., O'Boyle M., Wickramasinghe H. K., *Ultramicroscopy* **42-44** (1992) 268.

[6] Weaver J. M. R., Abraham D. W., *J Vac Sci Technol* **B 9** (1991) 1559 and references which are therein.

[7] Huang Y. J., Slinkman J., Williams C., *Ultramicroscopy* **42-44** (1992) 298.

[8] Sze S., The Physics of Semiconductor Devices (Wiley, New York, 1981)

[9] All these crossover limits have to be understood as a rough estimate since there are evaluated as a condition to obtain equality between the two right terms in equation (3). These limits depend on V_0 in the discussion, for each $Q_S(V_S)$ regime, we have selected the higher values obtained for the allowed V_0 values.